

## Study of the decay mode $\phi \rightarrow \pi^0 \pi^0 \gamma$ at SND

M.N. Achasov, S.E. Baru, K.I. Beloborodov, A.V. Berdyugin, A.V. Bozhenok, D.A. Bukin, S.V. Burdin, T.V. Dimova, V.P. Druzhinin, M.S. Dubrovin, I.A. Gaponenko, V.B. Golubev, V.N. Ivanchenko<sup>a</sup>, I.A. Koop, A.A. Korol, S.V. Koshuba, E.V. Pakhtusova, E.A. Perevedentsev, E.E. Pyata, A.A. Salnikov, S.I. Serednyakov, V.V. Shary, Yu.M. Shatunov, V.A. Sidorov, Z.K. Silagadze, Yu.V. Usov, A.V. Vasiljev

<sup>a</sup>Corresponding author, e-mail: V.N.Ivanchenko@inp.nsk.su

In the SND experiment at VEPP-2M  $e^+e^-$  collider the  $\phi(1020) \rightarrow \pi^0 \pi^0 \gamma$  decay was studied. Its branching ratio  $B(\phi \rightarrow \pi^0 \pi^0 \gamma) = (1.14 \pm 0.10 \pm 0.12) \cdot 10^{-4}$  was measured. It was shown, that  $f_0(980)\gamma$  mechanism dominates in this decay. The structure of the  $f_0(980)$  meson is discussed.

### 1. Introduction

First search for  $\phi \rightarrow \pi^0 \pi^0 \gamma$  decay was carried out with the ND detector at VEPP-2M  $e^+e^-$  collider in 1987 [1,2]. In this early experiment the upper limit  $B(\phi \rightarrow \pi^0 \pi^0 \gamma) < 10^{-3}$  was imposed. As it was shown later by N.Achasov [3], study of this decay can provide a unique information on the structure of the  $f_0(980)$  meson. Subsequent studies [4–9] proved this idea. In these works different models of the  $f_0(980)$ -meson structure were considered. The most popular were 2-quark model [10], 4-quark MIT-bag model [11], and  $K\bar{K}$  molecular model [6].

The study of radiative decays of  $\phi(1020)$  was one of the main goals of the new Spherical Non-magnetic Detector (SND) [12,13] which has been designed in Novosibirsk. It has better hermeticity, granularity, energy, and spatial resolution than the previous ND detector [2]. In 1995 SND started operation at VEPP-2M. In 1996 the PHI96 experiment to study  $\phi$  decays was carried out [14]. The total integrated luminosity of  $3.9 \text{ pb}^{-1}$  was collected which corresponds to about  $8 \cdot 10^6$  produced  $\phi$ -mesons. First indications of the reaction

$$e^+e^- \rightarrow \phi \rightarrow \pi^0 \pi^0 \gamma \quad (1)$$

were seen by SND in 1997 [15] on the basis of half statistic of PHI96. It was shown that  $f_0(980)\gamma$  mechanism of the  $\phi$ -meson decay dominates. At the same time CMD2 collaboration performed a search of the process  $\phi \rightarrow f_0(980)\gamma \rightarrow \pi^+\pi^-\gamma$  [16] but only a new upper limit was imposed. After completing the analysis of PHI96 experiment the results were publication [17]. In 1998 CMD2 [18] confirmed the existence of the reaction (1). At the same time the new experiment PHI98 [19] has been performed at VEPP-2M with the integrated luminosity  $6.0 \text{ pb}^{-1}$  which corresponding to about  $12 \cdot 10^6$   $\phi$  mesons produced. In this work the current status of the SND study of the process

(1) is reported.

### 2. Data analysis

Main resonant background to the decay (1) comes from the process

$$e^+e^- \rightarrow \phi \rightarrow \eta\gamma \rightarrow 3\pi^0\gamma \quad (2)$$

due to the merging of photons and/or loss of photons through the openings in the calorimeter. The main source of non-resonant background is a process

$$e^+e^- \rightarrow \omega\pi^0 \rightarrow \pi^0\pi^0\gamma. \quad (3)$$

The background from the  $\phi \rightarrow \rho\pi^0 \rightarrow \pi^0\pi^0\gamma$  decay is small [5,20], nevertheless its amplitude was included into simulation of the process (3). The background from the QED  $5\gamma$ -annihilation process was estimated and found to be negligible. The  $\phi \rightarrow K_S K_L \rightarrow \pi^0\pi^0 K_L$  decay can contribute due to nuclear interactions of  $K_L$  mesons in the material of the calorimeter but the process is suppressed by our cuts.

After applying cuts described in details in Ref.[17] the sample of  $\pi^0\pi^0\gamma$  events was selected in the PHI96 experiment. In the energy region of this experiment the invariant mass of the pion pair in the process (3) is less than  $700 \text{ MeV}$ . In the events satisfying this condition clear  $\omega(782)$  peak is seen in  $m_{\pi\gamma}$  distribution (Fig.1), proving the dominance of the process (3) in this kinematic region. The  $m_{\pi\gamma}$  parameter was defined as an invariant mass of the recoil photon and one of  $\pi^0$  mesons, closest to the  $\omega$ -meson mass. The 499 found events with  $750 \text{ MeV} < m_{\pi\gamma} < 815 \text{ MeV}$  were assigned to  $\omega\pi^0$  class, while 189 events with  $m_{\pi\gamma}$  outside this interval and  $m_{\pi\pi} > 700 \text{ MeV}$  were assigned to  $\pi^0\pi^0\gamma$  class. Subtracting the calculated contribution of the process (2) and using estimated probabilities of events misidentification for the processes (1) and (3), the number of the

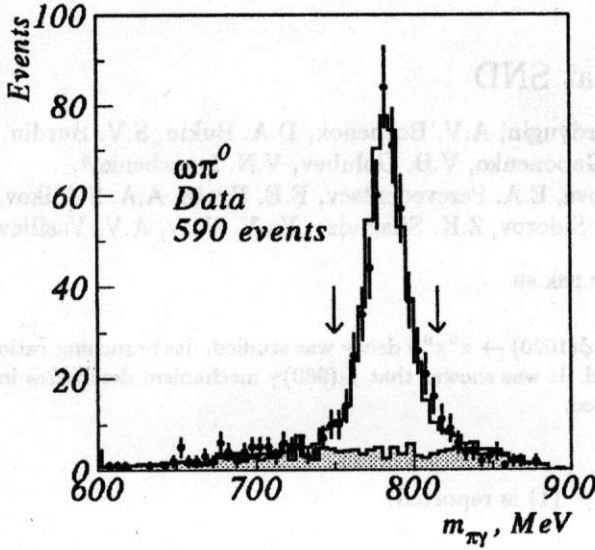


Figure 1. Distribution of  $\pi^0\gamma$  invariant mass for  $m_{\pi\pi} < 700 \text{ MeV}$ . Points - data, histogram - simulation, shaded histogram - sum of simulated contributions from  $\phi \rightarrow \eta\gamma$  and  $\phi \rightarrow \pi^0\pi^0\gamma$  decays, arrows - selection of the  $\omega\pi^0$  class.

events of the process (3) in the  $\omega\pi^0$  class was estimated to be equal to 449. The corresponding number of events of the decay (1) in the  $\pi^0\pi^0\gamma$  class is 164. The background from the process (3) was estimated using events of the  $\omega\pi^0$  class. No additional knowledge of the actual production cross section of this process was necessary.

For the events of the  $\pi^0\pi^0\gamma$  and  $\omega\pi^0$  classes the comparison of experimental and simulated distributions in  $\psi$  and  $\theta$  angles was done. The  $\psi$  is an angle of the recoil photon with respect to pion direction in the  $\pi^0\pi^0$  center of mass reference frame,  $\theta$  is an angle between recoil photon and the beam. The distribution of  $\theta$  for  $\pi^0\pi^0\gamma$  events with pion pair in a scalar state must be proportional to  $1 + \cos^2\theta$  and uniform in  $\cos\psi$ . The comparison (Fig.2a,c) shows, that in the  $\pi^0\pi^0\gamma$  class pions are actually produced in the scalar state. On the contrary, the experimental events of the  $\omega\pi^0$  class (Fig.2b,d) well match the hypothesis of the intermediate  $\omega\pi^0$  state with quite different  $\psi$  distribution. In addition, the spectrum was obtained (Fig.3) of the photon with the smallest energy in an event from the  $\pi^0\pi^0\gamma$  class, which demonstrate good coincidence between the data and the simulation.

The  $\pi^0\pi^0$  invariant mass distribution for the events with  $m_{\pi\gamma}$  outside the  $750 \text{ MeV} < m_{\pi\gamma} < 815 \text{ MeV}$  interval (Fig.4a) shows significant ex-

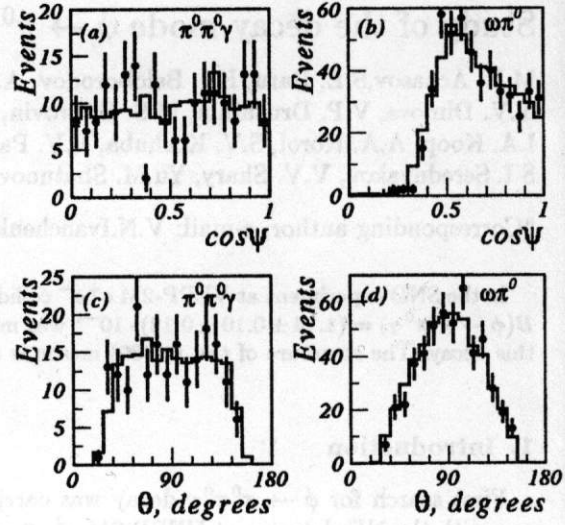


Figure 2. a, b - cosine of  $\psi$ , the angle between directions of  $\pi^0$  and recoil  $\gamma$  in the rest frame of  $\pi^0\pi^0$  system; c, d - distributions of  $\theta$ , angle of the recoil  $\gamma$  with respect to the beam. Points - data, histogram - simulation.

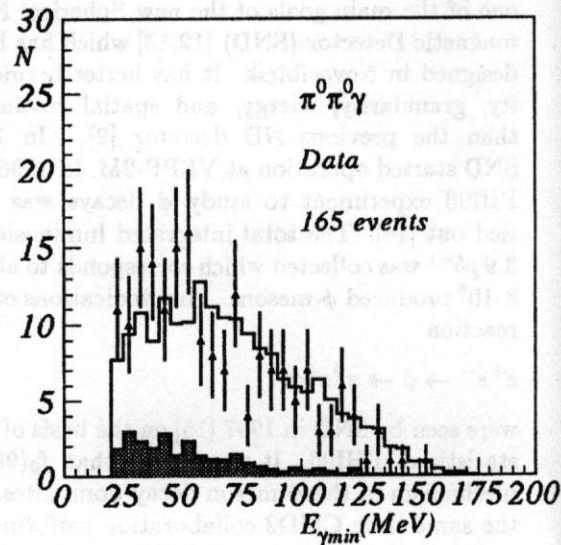


Figure 3. The energy deposition of the photon with the minimal energy in an event of the  $\pi^0\pi^0\gamma$  class. Points - data, histogram - simulation, shaded histogram - estimated background contribution from  $e^+e^- \rightarrow \omega\pi^0$  and  $\phi \rightarrow \eta\gamma$ .

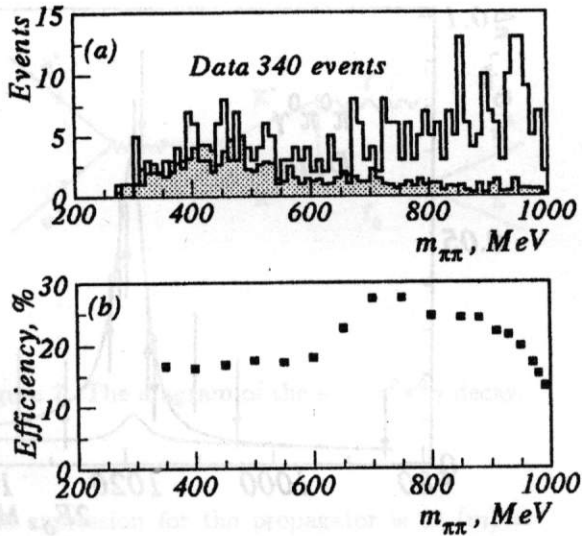


Figure 4. a - invariant mass distribution of  $\pi^0\pi^0$  pairs for selected  $\pi^0\pi^0\gamma$  events without acceptance corrections. Histogram - data, shaded histogram - estimated background contribution from  $e^+e^- \rightarrow \omega\pi^0$  and  $\phi \rightarrow \eta\gamma$ ; b - detection efficiency for  $\pi^0\pi^0\gamma$  events.

cess over background at large  $m_{\pi\pi}$ . At  $m_{\pi\pi} < 600$  MeV the sum of background contributions dominates. The detection efficiency (Fig.4b) for the process (1) was determined using simulation of the process  $\phi \rightarrow S\gamma \rightarrow \pi^0\pi^0\gamma$ , where  $S$  is a scalar state with a mass ranging from 300 to 1000 MeV and zero width. In addition, this simulation provided information on  $\pi^0\pi^0$  invariant mass resolution and event misidentification probability as a function of  $m_{\pi\pi}$ .

After background subtraction, correction for detection efficiency, and correction for misidentification, the mass spectrum was obtained (Fig.5). For masses in the (600–850) MeV interval the invariant mass resolution is equal to 12 MeV, so the 20 MeV bin size was chosen. At higher masses the resolution improves, reaching 7.5 MeV at 950 MeV, thus the bin size of 10 MeV was used for higher masses.

To check the accuracy of the detection efficiency, obtained from simulation, events of the process (2) with 7 photons in the final state and three reconstructed  $\pi^0$  mesons were analyzed [21]. All other selection criteria were the same as in the  $\pi^0\pi^0\gamma$  analysis. The number of observed events of the process (2) together with the PDG Table value for  $B(\phi \rightarrow \eta\gamma) = (1.26 \pm 0.06) \%$  [22] and known total integrated luminosity provided inde-

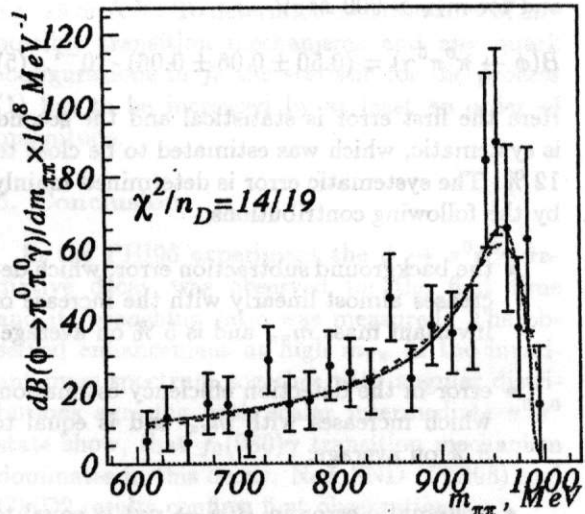


Figure 5. The measured  $\pi^0\pi^0$  invariant mass spectrum. Background is subtracted and efficiency corrections applied. Points - data, solid line - the result of the "broad resonance" fit, dashed line - the result of the "narrow resonance" fit.

pendent efficiency estimation, based on the data. Obtained 10% difference between experimental and simulated detection efficiencies was used as a correction to the  $\pi^0\pi^0\gamma$  detection efficiency, obtained from simulation. Such an approach minimizes systematic errors corresponding to inaccurate simulation of tails of distributions, used for event selection.

To monitor the stability of experimental results, the number of  $\pi^0\pi^0\gamma$  events was checked separately in all 7 experimental runs of PHI96. The results for all runs agree well within statistical uncertainty. Another important proof of validity of the results is the study of the process (2) [21], whose properties are very close to the decay under study. The preliminary analysis of the PHI98 data shows a qualitative agreement with the results of the PHI96 experiment. The difference between these experiments comes from two main factors: upgrade of the calorimeter electronics before PHI98 and higher trigger rate in PHI98.

### 3. Results

Summing data from the Fig.5 one can estimate branching ratio of the decay (1) for the mass range  $m_{\pi\pi} > 700$  MeV

$$B(\phi \rightarrow \pi^0\pi^0\gamma) = (1.00 \pm 0.07 \pm 0.12) \cdot 10^{-4}, \quad (4)$$

and for  $m_{\pi\pi} > 900 \text{ MeV}$

$$B(\phi \rightarrow \pi^0 \pi^0 \gamma) = (0.50 \pm 0.06 \pm 0.06) \cdot 10^{-4}. \quad (5)$$

Here the first error is statistical and the second is systematic, which was estimated to be close to 12%. The systematic error is determined mainly by the following contributions:

- the background subtraction error, which decreases almost linearly with the increase of invariant mass  $m_{\pi\pi}$  and is 5% on average;
- error in the detection efficiency estimation, which increases with  $m_{\pi\pi}$  and is equal to 8% on average;
- systematic error in  $B(\phi \rightarrow \eta\gamma)$  is equal to 5%.

The  $m_{\pi\pi}$  invariant mass spectrum (Fig.5) was fitted according to Refs.[3] and further used for the simulation of the decay (1). As a result the detection efficiency of the process (1) was estimated (14.72%) for invariant masses within the (600 – 1000) MeV interval (Fig.4a). This efficiency was used in the fitting of the  $\phi$ -resonance excitation curve. The visible cross section in each energy point  $\sigma_{vis}(s)$  was described as a sum of the processes (1), (2), and (3) with efficiency and radiative corrections taken into account for each process. The background cross section due to the process (3) was estimated by fitting the visible cross section of the events of the  $\omega\pi^0$  type with a linear function. The background from the process (2) was obtained from the simulation. The only free parameter of the fit was the  $\phi \rightarrow \pi^0 \pi^0 \gamma$  branching ratio, all other  $\phi$ -meson parameters were taken from the PDG data [22]. As a result (Fig.6), the following value was obtained:

$$B(\phi \rightarrow \pi^0 \pi^0 \gamma) = (1.14 \pm 0.10 \pm 0.12) \cdot 10^{-4}, \quad (6)$$

which, in contrast with (4) and (5), is valid for the whole mass spectrum. In the systematic error estimation the following considerations were taken into account. In comparison with the results (4) and (5) the accuracy of normalization 3% and efficiency estimation 5% are higher here, the background subtraction error 5% is the same, but an additional systematic error 6% exists, due to uncertainty in extrapolation of the invariant mass spectrum into the region  $m_{\pi\pi} < 600 \text{ MeV}$ . Smaller systematic uncertainty has a ratio of branching ratios:

$$\frac{B(\phi \rightarrow \pi^0 \pi^0 \gamma)}{B(\phi \rightarrow \eta\gamma)} = (0.90 \pm 0.08 \pm 0.07) \cdot 10^{-2}, \quad (7)$$

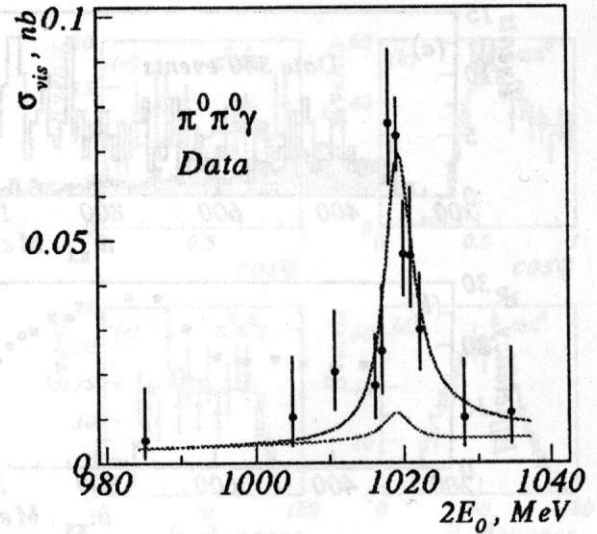


Figure 6. Energy dependence of the visible  $e^+e^- \rightarrow \pi^0 \pi^0 \gamma$  cross section. Points – data, solid line – fit, dotted line – estimated background contribution from  $e^+e^- \rightarrow \omega\pi^0$  and  $\phi \rightarrow \eta\gamma$ .

#### 4. Discussion

We would like to emphasize that all results presented in the previous section are not based on model assumptions about  $f_0$  structure. The enhancement at large  $m_{\pi\pi}$  (Fig.5) is compatible only with a large  $f_0\gamma$  contribution. Assuming that the process (1) is fully determined by  $f_0\gamma$  mechanism, using the relation  $B(f_0 \rightarrow \pi^+\pi^-) = 2B(f_0 \rightarrow \pi^0\pi^0)$ , and neglecting the decay  $\phi \rightarrow KK\gamma$  [3], we can obtain from (6)

$$B(\phi \rightarrow f_0(980)\gamma) = (3.42 \pm 0.30 \pm 0.36) \cdot 10^{-4}. \quad (8)$$

Further analysis is carried out without this assumption. The intermediate states in the decay (1) are  $f_0\gamma$  and  $\sigma\gamma$  [20]. In that case the mass spectrum can be described by the following expression:

$$\frac{dBr(\phi \rightarrow \pi^0 \pi^0 \gamma)}{dm_{\pi\pi}} = \frac{2m_{\pi\pi}^2 \Gamma(\phi \rightarrow f_0\gamma) \Gamma(f_0 \rightarrow \pi^0 \pi^0)}{\pi \Gamma_\phi} \left| \frac{1}{D_f(m_{\pi\pi})} + \frac{A_\sigma \cdot e^{i\varphi_\sigma}}{D_\sigma(m_{\pi\pi})} \right|^2 \quad (9)$$

where  $D_s(m_{\pi\pi})$  is a scalar meson propagator,  $\Gamma(f_0 \rightarrow \pi^0 \pi^0)$  and  $\Gamma(\phi \rightarrow f_0\gamma)$  are functions of  $m_{\pi\pi}$ ,  $A_\sigma = g_{\sigma\pi\pi} g_{\phi\sigma\gamma} / g_{f_0\pi\pi} g_{f_0\gamma}$  takes into account contribution from  $\sigma$ -meson. The width of decay of the scalar meson can be written as

$$\Gamma(f_0 \rightarrow \pi^0 \pi^0) = \frac{g_{f_0\pi^+\pi^-}^2}{32\pi m_{\pi\pi}} \sqrt{1 - \frac{4m_{\pi^0}^2}{m_{\pi\pi}^2}}. \quad (10)$$

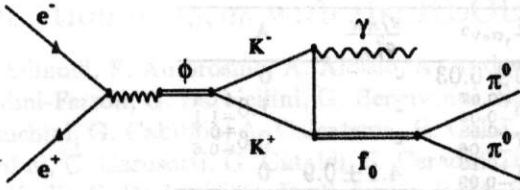


Figure 7. The diagram of the  $\phi \rightarrow \pi^0 \pi^0 \gamma$  decay.

The expression for the propagator is  $D_x(m) = m_x^2 - m^2 - i \cdot m \Gamma_x(m)$ . Because the decay mode  $f_0 \rightarrow K\bar{K}$  is negligible in the mass range of interest (Fig.5) the relation  $\Gamma_f(m) = 3\Gamma(f_0 \rightarrow \pi^0 \pi^0)$  is used for the  $f_0$  propagator. The  $\sigma$ -meson parameters were fixed according to Ref.[20]  $m_\sigma = 1 \text{ GeV}$ ,  $\Gamma_\sigma = 800 \text{ MeV}$ ,  $\varphi_\sigma = 0$ .

In the "narrow resonance" approximation [23] the width  $\Gamma(\phi \rightarrow f_0 \gamma)$  depends on the coupling constant  $g_{\phi f_0 \gamma}$ . But this simple approximation seems inadequate for  $f_0$  meson. In decay under study the width corrections might be very large [23]. Instead of calculating such corrections we used complete formulas from Ref.[3] for the "broad resonance" fit which are based on the diagram with kaon triangle (Fig.7). In this case the width  $\Gamma(\phi \rightarrow f_0 \gamma)$  depends on the product  $g_{\phi K\bar{K}} \cdot g_{f_0 K\bar{K}}$ .

The results of the fit are presented in Table 1. Comparison of the results of the fits shows a strong model dependence of  $f_0$ -meson parameters. The statistic accuracy does not allow to define the level of the amplitude of  $\sigma$  in (9). At the same time fitting curves in Fig.5 practically coincide. Of course, the "broad resonance" parameterization looks more realistic. In this case the value of the coupling constant  $g_{f_0 K\bar{K}}^2/4\pi = 2.13$  obtained from the fit agrees with the predictions of 4-quark MIT-bag model ( $2.3 \text{ GeV}^2$  [3,11]) as well as the value of the branching ratio (8). The corresponding predictions of the  $K\bar{K}$  molecular model ( $0.6 \text{ GeV}^2$  [6,20]) and the 2-quark model ( $0.3 \text{ GeV}^2$  [3]) are lower. Of course, there is an open question: what is the precision of the predictions?

Thus, the measured  $\phi \rightarrow f_0 \gamma$  branching ratio and coupling constants are higher than 2-quark and  $K\bar{K}$  model predictions, that can be considered as another indication of significant 4-quark MIT-bag part in the  $f_0$  meson not excluding partial contribution from other quark configurations,

e.g.  $s\bar{s}$  or  $K\bar{K}$ . To determine contributions of any possible transition mechanisms and any quark configurations in  $f_0$  the statistic for the process (1) has to be increased by at least an order of magnitude.

## 5. Conclusion

In the PHI96 experiment the  $\phi \rightarrow \pi^0 \pi^0 \gamma$  radiative decay was observed for the first time and its branching ratio was measured. The observed enhancement at high  $m_{\pi\pi}$  in the invariant mass spectrum together with angular distributions agreeing with scalar intermediate  $\pi^0 \pi^0$  state show, that  $f_0(980)\gamma$  transition mechanism dominates in this decay. New SND (PHI98) and CMD2 results confirm first observation.

The measured  $f_0$  parameters are strongly model dependent due to the fact that  $f_0$  meson is broad and its mass is close to  $K\bar{K}$  threshold, making simple Breit-Wigner description of the resonance inadequate.

The observed high decay probability  $\sim 10^{-4}$  gives evidence, that  $f_0$  meson contains significant 4-quark component.

## 6. Acknowledgement

The work is partially supported by RFBR (Grants No 99-02-16813) and STP "Integration" (Grant No 274).

## REFERENCES

1. V.P.Druzhinin et al., Z. Phys. C, 1987, vol. 37, p. 1.
2. S.I.Dolinsky et al., Phys. Reports, 1991, vol. 202, p. 99.
3. N.N.Achasov, V.N.Ivanchenko, Nucl. Phys. B, 1989, vol. 315, p. 465.
4. J.Weinstein, N.Isgur, Phys. Rev. D, 1990, vol. 41, p. 2236.
5. A.Bramon, A.Grau, G.Panchieri, Phys. Lett. B, 1992, vol. 283, p. 416.
6. F.E.Close, N.Isgur, S.Kumano, Nucl.Phys. B, 1993, vol. 389, p. 513.
7. N.Broun, F.E.Close, The second DAΦNE Physics Handbook, vol. 2, Frascati: INFN Frascati, 1995, p. 649.
8. A.Bramon, M.Greco, ibid, p. 663.
9. J.L.Lucio, M.Napsuciale, Phys. Lett. B, 1994, vol. 331, p. 418.
10. N.A.Törnqvist, Phys. Rev. Lett., 1982, vol. 49, p. 624.
11. R.L.Jaffe, Phys. Rev. D, 1977, vol. 15, p. 267.
12. V.M.Aulchenko et al., Proc. of Second Workshop on physics and detectors for DAΦNE, Frascati, Italy, April 4-7, 1995, p.605.

Table 1  
The results of the fit of two pion mass spectrum for the  $\phi \rightarrow \pi^0 \pi^0 \gamma$  decay for different models.

Model	$m_f, \text{MeV}$	$\Gamma_f, \text{MeV}$	$\frac{g_{fKK}^2}{4\pi}, \text{GeV}^2$	$\frac{g_{f\pi\pi}^2}{4\pi}, \text{GeV}^2$	$\frac{g_{fKK}^2}{g_{f\pi\pi}^2}$	A
Narrow	$984 \pm 12$	$74 \pm 12$	-	$0.20 \pm 0.03$	-	0
Narrow	$968^{+12}_{-7}$	$61^{+26}_{-19}$	-	$0.16^{+0.07}_{-0.05}$	-	$1.8^{+1.4}_{-1.1}$
Narrow/Wide	$987^{+7}_{-9}$	$98^{+29}_{-22}$	-	$0.27^{+0.08}_{-0.06}$	-	$0.6^{+0.7}_{-0.6}$
Wide	$970 \pm 6$	$188^{+48}_{-33}$	$2.13^{+0.89}_{-0.56}$	$0.51^{+0.13}_{-0.09}$	$4.1 \pm 0.9$	0
PDG98 [22]	$980 \pm 10$	40-100				

13. V.M.Aulchenko et al., Preprint IYF 99-16, Novosibirsk, 1999.
14. M.N. Achasov et al., In: Proc. at 7th Inter. Conf. on Hadron Spectroscopy (Hadron'97), Upton, NY, 25-30 Aug 1997, p.26; Budker- INP 97-78, Sep 1997; e-Print Archive: hep-ex/9710017.
15. M.N.Achasov et.al., Proc. of HADRON97, Upton, NY, August 24-30, 1997, p.783; e-Print hep-ex/9711023; To be published in Phys. Atom. Nucl., 1999.
16. R.R. Akhmetshin et al., Phys. Lett. B, 1997, vol. 415, p. 452.
17. M.N.Achasov et al., Phys. Lett. B, 1998, vol. 440, p. 442.
18. R.R. Akhmetshin et al., Budker INP 99-11, Feb 1999; Novosibirsk, 1999.
19. M.N. Achasov et al., Budker INP 98-65, Sep 1998; e-Print Archive: hep-ex/9809013.
20. N.N.Achasov, V.V.Gubin, Phys. Rev. D, 1997, vol. 56, p. 4084.
21. M.N.Achasov et al., e-Print: hep-ex/9809002; Pis'ma v ZhETF (JETP Lett.), 1998, vol. 68, p. 549.
22. C.Caso et al. (Particle Data Group), Europ. Phys. Jour. C, 1998, vol.3 p. 1.
23. N.N.Achasov, V.V.Gubin, Phys. Lett. B, 1995, vol. 363, p. 106.

